Artemisia annua L. extracts prevent *in vitro* replication of SARS-CoV-2

Nair[1], M.S., Huang[1], Y., Fidock[2,3], D.A., Polyak[4], S.J., Wagoner[4], J., Towler[5], M.J., Weathers[5#], P.J.

[1]Aaron Diamond AIDS Research Center, Columbia University Vagelos College of Physicians and Surgeons, New York, NY, USA.

[2]Department of Microbiology and Immunology, Department of Medicine, Columbia University Irving Medical Center, New York, NY 10032, USA.

[3]Division of Infectious Diseases, Department of Medicine, Columbia University Irving Medical Center, New York, NY 10032, USA.

[4]Department of Laboratory Medicine and Pathology, University of Washington, Seattle, WA, 98104

[5]Department of Biology and Biotechnology, Worcester Polytechnic Institute, Worcester, MA 01609, USA.

Corresponding author:

Pamela Weathers

Department of Biology and Biotechnology

Worcester Polytechnic Institute

100 Institute Rd

Worcester, MA 01609 USA

Email: weathers@wpi.edu

Phone: 508-831-5196

FAX: 508-831-6362

ABSTRACT:

SARS-CoV-2 (Covid-19) globally has infected and killed millions of people. Besides remdesivir, there are no approved small molecule-based therapeutics. Here we show that extracts of the medicinal plant, *Artemisia annua* L., which produces the antimalarial drug artemisinin, prevents SARS-CoV-2 replication in vitro. We measured antiviral activity of dried leaf extracts of seven cultivars of *A. annua* sourced from four continents. Hot-water leaf extracts based on artemisinin, total flavonoids, or dry leaf mass showed antiviral activity with IC_{50} values of 0.1-8.7 µM, 0.01-0.14 µg, and 23.4-57.4 µg, respectively. One sample was >12 years old, but still active. While all hot water extracts were effective, concentrations of artemisinin and total flavonoids varied by nearly 100-fold in the extracts and antiviral efficacy was inversely correlated to artemisinin and total flavonoid contents. Artemisinin alone showed an estimated IC_{50} of about 70 µM, and antimalarial artemisinin derivatives artesunate, artemether, and dihydroartemisinin were ineffective or cytotoxic at elevated micromolar concentrations. In contrast, the antimalarial drug amodiaquine had an IC_{50} = 5.8 µM. The extracts had minimal effects on infection of Vero E6 or Calu-3 cells by a reporter virus pseudotyped by the SARS-CoV-2 spike protein. There was no cytotoxicity within an order of magnitude of the antiviral IC_{90} values. Results suggest the active component in the extracts is likely something besides artemisinin or is a combination of components acting synergistically to block post-entry viral infection. Further studies will determine in vivo efficacy to assess whether *A. annua* might provide a cost-effective therapeutic to treat SARS-CoV-2 infections.

KEY WORDS: *Artemisia annua*, artemisinin, SARS-Cov-2, Covid-19, artesunate, artemether, amodiaquine, dihydroartemisinin

INTRODUCTION:

The global pandemic of SARS-CoV-2 (the etiologic agent of COVID-19) has infected over 80 million people and killed nearly 1.8 million as of December 29, 2020 (https://coronavirus.jhu.edu/). There is an intense effort to distribute the registered Pfizer/BioNTech and Moderna vaccines, but to our knowledge, there is no approved therapeutic and global infections keep rising with the sporadic advent of new variants.

The medicinal plant *Artemisia annua* L. produces the antimalarial therapeutic artemisinin, a sesquiterpene lactone produced and stored in the glandular trichomes located on the shoots and especially the leaves and flowers of the plant. Both the plant and artemisinin have been used safely for over 2,000 years to treat a variety of ailments, especially malaria. Artemisinin derivatives (Figure 1) are front-line therapeutics for treating malaria and are delivered with a second antimalarial drug, such as lumefantrine or amodiaquine, which are formulated as artemisinin-based combination therapies (Blasco et al. 2017). Artemisinins also have some antiviral activity (Efferth 2018). Extracts of *A. annua* showed anti-SARS-CoV-1 activity, suggesting that they may be active against SARS-CoV-2 (Li et al. 2005).

Artemisinin delivered *per os* from *A. annua* consumption is highly bioavailable and distributes through peripheral blood and into a plethora of organs including lungs, liver, heart, and brain (Desrosiers et al. 2020). Furthermore, both artemisinins and the plant *A. annua* reduce levels of inflammatory cytokines including IL-6 and TNF-α *in vivo* (Desrosiers et al. 2020; Hunt et al. 2015; Shi et al. 2015). These effector molecules can be problematic during the "cytokine storm" suffered by many SARS-CoV-2 patients (Schett et al. 2020). Artemisinin also blunts fibrosis (Larson et al.

2019; Dolivo et al. 2020), another problem experienced by SARS-CoV-2 survivors that causes more lasting damage to organs (Lechowicz et al. 2020; Liu et al. 2020a). A recent report showed that a number of artemisinin-related compounds have some anti-SARS-CoV-2 activity, with dihydroartemisinin, artesunate, and arteannuin B having IC_{50} values <30 µM (Cao et al. 2020), and dihydroartemisinin ACTs with 1-10 µM IC_{50}s (Bae et al. 2020). Artesunate was reported to have IC_{50} values against SARS-CoV-2 of 7-12 µg/mL (0.7-1.2 µM; Gilmore et al. 2020) and 2.6 µM (Bae et al. 2020). Knowing that artemisinin is much more bioavailable *per os* when delivered via *A. annua* (Weathers et al. 2011; Weathers et al. 2014; Desrosiers et al. 2020), we posited that encapsulated powdered dried leaves of *A. annua* may be a safe, cost-effective therapeutic to combat SARS-CoV-2 infections. Here we report *in vitro* results from testing extracts of a diversity of *A. annua* cultivars against SARS-CoV-2 propagated in Vero E6 cells, with correlation analyses of antiviral efficacy to artemisinin and total flavonoid contents.

METHODS:

Plant material, extract preparations, and artemisinin and total flavonoid analyses: Batches of dried leaves of various cultivars of *Artemisia annua* L. with source, age, and voucher identity when known are shown in Table 1. Hot-water extracts (tea infusions) were prepared as follows: dried leaves at 10 g/L were added to boiling water on a stir plate and boiled for 10 min, then poured through a 2 mm stainless steel sieve to retain most solids. Extracts were then cooled and sterile-filtered (0.22 µm) prior to being stored at -20°C. Dichloromethane (DCM) extracts of dried leaves were also prepared by extraction of 25 mg in 4 mL DCM for 30 min in a sonicating water bath (Fischer Scientific FS60, 130 W), separating solvent from solids with Pasteur pipets, drying under nitrogen flow, and storing at -20°C until analyzing for artemisinin using gas chromatography / mass

93 spectrometry, as detailed in Martini et al. (2020). For artemisinin analysis of tea infusions, two-
94 phase overnight aliquots extracted in DCM in a 1:1 ratio were separated by using Pasteur pipets,
95 dried under nitrogen flow, and stored at -20°C until analysis as previously noted (Martini et al.
96 2020). Total flavonoids were analyzed in DCM extracts via the aluminum chloride method of
97 Arvouet-Grand et al. (1994) and were quantified as quercetin equivalents. Artemisinin and total
98 flavonoid contents of tea infusions are shown in Table 2. The DCM extract of *A. annua* (cv SAM)
99 contained a total of 34 mg of artemisinin. After solubilizing in PEG400 containing 5% DMSO0 the
100 concentration was 8.95 mg/mL.
101
102 **Viral culture and analyses:** Vero E6 cells, obtained from the American Type Culture collection
103 (ATCC CRL-1586), were cultured in Minimal Essential Eagle Medium (EMEM) containing penicillin-
104 streptomycin (1x 100 U/mL) and 10% fetal calf serum. SARS-CoV-2 isolate USA/WA1 was from BEI
105 Resources (www.beiresources.org). We infected Vero E6 cells with the USA/WA1 isolate according
106 to Liu et al. (2020b). Briefly, infected cells were incubated in flasks until a viral cytopathic effect
107 was observed. The supernatant was then harvested and titered for its tissue culture infective dose
108 (TCID) using an end point dilution method. TCID was calculated using the Reed Muench
109 proportional distance method (Reed and Muench 1938). Viral aliquots were frozen, then later
110 thawed and used for infection experiments at their desired infectivity (multiplicity of infection
111 (MOI).
112
113 **Assays for determining drug inhibition of SARS-CoV-2:** Except for tea infusions that were diluted
114 in water and used directly, amodiaquine, artesunate, artemether, artemisinin, deoxyartemisinin,
115 and dihydroartemisinin compounds were solubilized and diluted in 5% DMSO in PEG400 or 5%

DMSO in EMEM enriched with fetal calf serum at a final concentration of 7.5%, prior to testing for efficacy against SARS-CoV-2. Indicated dilutions of the drug were incubated for 1 h in wells of 96 well tissue culture plates containing a monolayer of Vero E6 cells seeded the day before at 20,000 cells/well. Post incubation of the drug with the cells, SARS-CoV-2 USA/WA1 virus was added to each well at a multiplicity of infection of 0.1. Cells were cultured for 3 days at 37°C in 5% CO_2 and scored for cytopathic effects as detailed in Liu et al. (2020b). Vesicular Stomatitis Virus (VSV)-spike pseudoviruses were generated as described (Hoffmann et al. 2020; Whitt 2010), using the spike gene from SARS-CoV-2 containing the D614G mutation (Korber et al. 2020). The construct also contains a deletion of 18 amino acids from the C-terminus, which facilitates loading onto pseudovirus particles. The construct (Δ18 D614G) was kindly provided by Markus Hoffmann and Stefan Pöhlmann (Leibniz-Institut für Primatenforschung, Germany). The day prior to infection, Vero E6 and Calu-3 cells (ATCC HTB-55) were plated in black, clear-bottomed plates at 10,000 and 30,000 cells/well, respectively, in a final volume of 90 µl. Cells were then treated with 10 µl of serially diluted *Artemisia* extract in water and incubated for 1 h prior to infection with 100 µl of VSV-spike Δ18 D614G pseudovirus. At 22 h post-infection, PrestoBlue was added 2 h before the end of assay, so that cell viability in parallel non-infected, drug-treated wells could be measured. Virus-produced Renilla luciferase activity was measured by Renilla-Glo assay at 24 h post-infection. Results were converted into percent of control. Drug concentrations were log transformed and the concentration of drug(s) that inhibited virus by 50% (*i.e.*, IC_{50}), and the concentration of drug(s) that killed 50% of cells (*i.e.*, CC_{50}), were determined via nonlinear logistic regressions of log(inhibitor) versus response-variable dose-response functions (four parameters) constrained to a zero-bottom asymptote by statistical analysis using GraphPad Prism 9 (GraphPad Software, Inc.) as described by Hulseberg et al. (2019).

Cell viability assay: To determine the viability of Vero E6 cells post drug treatment, cells were exposed to indicated doses of tea infusions diluted in EMEM containing fetal calf serum at a final concentration of 7.5%, and incubated at 37°C in 5% CO_2 for 24 h. Cells were then washed and treated with 100 µL XTT reagent premixed with activation agent, followed by incubation for another 2 h at 37°C in 5% CO_2. Culture medium was removed, and absorbance measured at 450 nm. The absorbance ratio of treated to untreated cells was plotted as percent viability. Imatinib, an FDA-approved apoptosis inducer and tyrosine kinase inhibitor, was used as a positive control.

Chemicals and reagents: Unless otherwise stated all reagents were from Sigma-Aldrich (St. Louis, MO) DCM was from ThermoFisher (Waltham, MA, USA); artemisinin was from Cayman Chemical (Ann Arbor, MI, USA); artemether, artesunate, and dihydroartemisinin were gifts from Prof. J. Plaizier-Vercammen (Brussels, Belgium); deoxyartemisinin was from Toronto Research Chemicals (North York, ON, Canada), amodiaquine HCl hydrate (Cat #: 562290) and imanitib (Cat # 100956) were from Medkoo Biosciences Inc. (Morrisville, NC, USA); EMEM (Cat # 30-2003) and XTT reagent (Cat # 30-1011k) were from ATCC; PrestoBlue was from Life Technologies (Cat #P50201); Renilla-Glo was from Promega (E2720).

Statistical analyses: All *in vitro* anti-SARS-CoV-2 analyses were done at least in triplicate. Plant extract analyses had n≥6 independent assays. IC_{50} and IC_{90} values were calculated using GraphPad Prism V8.0. Correlations between antiviral activity and artemisinin or total flavonoids used Spearman's Rho analysis (Spearman 1904).

RESULTS:

Artemisia annua hot water extracts have anti-SARS-CoV-2 activity. Hot water extracts of the *A. annua* cultivars used in the study had considerably different artemisinin contents ranging from 20.1 ± 0.8 to 149.4 ± 4.4 µg/mL (Table 2). Total flavonoid content of leaf material ranged from 7.3 ± 0.2 to 37.2 ± 0.7 µg/mL (Table 2). All cultivars showed anti-SARS-CoV-2 activity (Figure 2; Table 2), and IC_{50} values calculated on the basis of artemisinin or total flavonoid content ranged from 0.1-8.7 µM, or 0.01-0.14 µg/mL, respectively (Table 2). On the basis of leaf dry mass, IC_{50} values ranged from 13.5-57.4 µg dry weight (DW). On a µg artemisinin/mL tea basis, the IC_{50} of the samples ranged from 0.03 to 2.5 µg/mL. Analysis of frozen (SAM -20C) extracts remained potent upon thawing and reanalysis (Table 2, Figure 2). Leaf samples that were 12 years old were also active with an IC_{50} of 32.9 µg DW. Infection of Vero E6 or Calu-3 human lung cells by VSV-spike pseudoviruses was minimally inhibited by the extract, except perhaps at the highest dose tested of 500 µg/mL (Figure 3). Indeed, GraphPad Prism-calculated IC_{50}/CC_{50} values were 545/3564 µg/mL for Calu-3 and 410/810 µg/mL for Vero E6 cells.

Activity of antimalarials. In a separate analysis, DCM and hot water extracts of *A. annua* were compared, yielding IC_{50} values of 12.0 and 11.8 µM, respectively (Figure 4). However, due to solvent toxicity at higher concentrations of the drug on Vero E6 cells, the IC_{50} of the DCM extract had to be estimated. Similar solvent toxicity was encountered with artemisinin that subsequently was estimated to have an IC_{50} of 70 µM (Figure 4). Artemether efficacy was estimated at 1.23 µM but was cytotoxic at concentrations slightly above that level (Figure 4). Artesunate and dihydroartemisinin were inactive at <100 µM. In contrast, amodiaquine showed efficacy at 5.8 µM (Figure 4).

185

186 *Anti-SARS-CoV-2 activity of hot water extracts inversely correlated to artemisinin or total flavonoid*
187 *content*. A Spearman's Rho analysis showed that neither IC_{50} nor IC_{90} values of the hot water
188 extracts correlated to either artemisinin or total flavonoid content (Figure 5). Results of IC_{50} and
189 IC_{90} calculations based on dry leaf mass used to prepare the tea were tightly grouped (Figure 2).
190 Although cultivar IC_{50} ranking from most to least effective on dry weight basis was BUR, MED, A3,
191 #15, PEG01, SAM1, SAM2, and FLV5 (Table 2), the maximum differential was less than 44 µg DW of
192 dried leaves, or ~4.4 µL of tea infusion, an inconsequential difference.

193

194 **Hot water extracts are not cytotoxic.** When cytotoxicity of the hot water extracts to the Vero E6
195 cells was measured, cell viability did not substantially decrease (Figure 6A) at 24 h post treatment.
196 In comparison, the apoptotic inducer imatinib showed a dose-dependent decrease in viability of
197 the cells by 90% (Figure 6B). At the higher concentrations of hot water extracts, there appeared to
198 be proliferation of Vero E6 cells (Figure 6A).

199

200 *Human bioavailability*. To query the potential of using dried leaf *A. annua* (DLA) as a potential
201 therapeutic, we tracked artemisinin as a marker molecule post consumption of *per os* delivered
202 DLA in a human. One of us (PJW) consumed 3 g of encapsulated DLA of the SAM cultivar, had her
203 blood drawn at 2 and 5 h post consumption, and 7.04 and 0.16 µg artemisinin/mL serum,
204 respectively, were measured (See Supplemental Data). Thus, at 2 h post ingestion, 36% of the
205 original DLA-delivered artemisinin was detected in the serum, dropping to 0.8% at 5 h post
206 ingestion (See Supplemental data Table S1). This corresponded at 2 h to 2.35 µg artemisinin/mL
207 serum of DLA-delivered artemisinin per gram of DLA consumed.

208

209 **DISCUSSION:**

210 This is the first report of anti-SARS-CoV-2 efficacy of hot water extracts of a wide variety of
211 cultivars of *A. annua* sourced from four continents. These extracts had an IC_{50} corresponding to
212 <12 µM artemisinin, with DCM extracts of *A. annua* showing similar efficacy. In contrast,
213 artemisinin alone had an estimated IC_{50} about sixfold greater (~70 µM), suggesting the plant
214 extracts were more potent against SARS-CoV-2. Furthermore, the anti-SARS-CoV-2 effect was
215 inversely correlated to the artemisinin content of the extracts that varied by one to nearly two
216 orders of magnitude for IC_{50} and IC_{90} values. Total flavonoid content also was inversely correlated
217 to antiviral activity. One of the cultivar samples was obtained in 2008 and was still active at a level
218 comparable to the most recently harvested cultivar samples, suggesting that the active principle is
219 ubiquitous to different *A. annua* cultivars and chemically stable during long-term room
220 temperature dry storage. None of the plant extracts were cytotoxic to Vero 6 or Calu-3 cells at
221 concentrations approaching the IC_{50} or IC_{90} values. Finally, the minimal antiviral effects against VSV
222 pseudoviruses containing the SARS-CoV-2 spike protein suggests that *Artemisia* inhibits SARS-CoV-
223 2 infection primarily by targeting a post-entry step.

224

225 Although Cao et al. (2020) reported an EC_{50} of 10.28 µM for arteannuin B, a metabolite that is
226 formed in a side branch of the artemisinin biosynthetic pathway and that is often present in *A.*
227 *annua* extracts, only three of the tested tea extracts had any detectable arteannuin B with SAM
228 having 3.2 µg/mL. Arteannuin B in BUR and MED was barely detectable. Thus, arteannuin B was
229 eliminated as the principle active component, although if present in an extract, arteannuin B may
230 be providing some antiviral effect as part of the more complex plant extract mixture. Although

231 they can be present in substantial amounts in *A. annua* (Weathers and Towler 2014; Towler and
232 Weathers 2015; see supplemental Table S2), neither artemisinic acid nor deoxyartemisinin, also
233 metabolites in the artemisinin biosynthetic pathway, showed anti-SARS-CoV-2 activity in this
234 study.
235
236 There is some discrepancy among IC_{50} molar values in this and other studies for anti-SARS-CoV-2
237 efficacy (Table 3). In contrast to Bae, Cao, and Gilmore, we did not observe any anti-SARS-CoV-2
238 activity for artesunate or dihydroartemisinin. Artemether in our study had an IC_{50} of 1.23 µM,
239 while Cao et al. (2020) reported an EC_{50} of 73.8 µM but with less toxicity than we observed. In
240 particular, we noted cytotoxicity of artemether. The contrasts are likely the result of differences in
241 how we conducted our viral challenge experiments or solvents used to challenge the virus in Vero
242 E6 cells. For example, our study solubilized our pure artemisinin and other antimalarial
243 compounds in 5% DMSO in PEG400, while the other two studies solubilized compounds in DMSO.
244 Our preliminary experiments indicated that solubilizing in pure DMSO was too toxic to Vero cells
245 to achieve dosing of drug concentrations needed to obtain an IC_{50} value. In addition, Cao et al. also
246 had a different viral assay system. We used an endpoint assay to measure the cytopathic effect of
247 the replicating virus at 72 h and estimate the IC_{50} values while they collected supernatants to assay
248 the total RNA levels at 24 h post infection using RT-PCR. We recognize that such inherent
249 variations in the biological assays would offset the calculated values. Gilmore et al. (2020) also
250 tested a hot water extract of *A. annua* and observed EC_{50} values ranging from 260-390 µg/mL.
251 However, our hot water extracts are not directly comparable to those of Gilmore et al. because we
252 did not dry, concentrate, and then weigh our extracts. Furthermore, we extracted for 10 min in
253 boiling water, while they extracted for 200 min in boiling water. At present it is not possible to

compare our hot water extracts directly. In addition, different viruses were used in our study versus that of Gilmore et al., which could affect the inherent replication kinetics of the assay and in turn affect the specific IC_{50} numbers.

We and others noted there was anti-SARS-Cov-2 activity by other non-artemisinin antimalarial drugs including amodiaquine at an IC_{50} = 5.8 µM (this study), tafenoquine at an IC50 of 2.6 µM (Dow et al. 2020), and lumefantrine at a reported IC_{50} = 23.2 µM (Cao et al. 2020). Gendrot et al. (2020) also reported anti-SARS-CoV-2 activity of various ACTs drugs at doses used for treating malaria with mefloquine-artesunate (550 mg + 250 mg, respectively) providing the maximum inhibition, namely 72% of viral replication at serum C_{max}. Other combinations were less effective.

The high bioavailability of artemisinin after oral consumption of dried-leaf *A. annua* (DLA) was not surprising considering that a series of earlier studies in rodents showed the drug is >40 fold more bioavailable when delivered via the plant than in purified form (Weathers et al. 2011; Weathers et al. 2014). The increased bioavailability is mainly the result of three mechanisms: essential oils in the plant material improving the solubility of artemisinin, improved passage across the intestinal wall, and especially the inhibition of liver cytochrome P450s, 2B6, and 3A4 that are critical in first-pass metabolism (Desrosiers and Weathers 2016, 2018; Desrosiers et al. 2020). The anti-SARS-CoV-2 IC_{90} of the SAM1 and SAM2 cultivar samples ranged from 12.3-18.8 µM, equal to 1.7-2.6 µg/mL, so 1 g of the SAM cultivar delivered *per os* yielded 2.6 µg/mL in a patient's serum. Thus, 1 g of DLA could deliver enough artemisinin/DLA to achieve the IC_{90} of the hot water extract. While clearly human trials are required, these hypothetical estimations suggest that reasonable amounts of DLA consumed *per os* may be able to provide a cost-effective anti-SARS-CoV-2 treatment. Indeed, the

broad scale use of both artemisinin and non-artemisinin compound antimalarials including *A. annua* tea infusions across Africa may help in part explain why despite having anti-SARS-CoV-2 antibodies, Africans have not to date suffered the clinical scourge of SARS-CoV-2 like the rest of the world (Uyoga et al. 2020).

CONCLUSIONS:

This is a first report of the *in vitro* anti-SARS-CoV-2 activity of hot water extracts of *A. annua* wherein there was no cytotoxicity and where we showed reasonable levels of orally consumed plant material. If subsequent clinical trials are successful, *A. annua* could potentially serve as a safe therapeutic that could be provided globally at reasonable cost and offer an alternative to vaccines.

ACKNOWLEDGEMENTS:

Gratitude is extended to Tim Urekew (TJU Associates, NY, NY) and Scott Rudge (RMC Pharmaceutical Solutions, Inc, Longmont, CO), for their early advice and collaboration linkages. Prof. David Ho is gratefully acknowledged for supporting the live virus work in his lab. Award Number NIH-2R15AT008277-02 to PJW from the National Center for Complementary and Integrative Health funded phytochemical analyses of the plant material used in this study. The content is solely the responsibility of the authors and does not necessarily represent the official views of the National Center for Complementary and Integrative Health or the National Institutes of Health. SJP is partially supported by a Washington Research Foundation Technology Commercialization Phase 1 grant and NIH grant 3U41AT008718-07S1 from the National Center for Complementary and Integrative Health.

CONFLICT OF INTEREST STATEMENT:

Authors declare they have no competing conflicts of interest in the study.

AUTHOR CONTRIBUTIONS:

MSN – conducted SARS-CoV-2 experiments, helped analyze the data, and contributed to the manuscript.

YH – conducted SARS-CoV-2 experiments, helped analyze the data, and contributed to the manuscript.

DAF – provided reagents, helped analyze the data, and edited the manuscript.

SJP – helped plan and analyze pseudovirus data, and contributed to manuscript

JW – conducted pseudovirus experiments, helped analyze data, and contributed to manuscript

MJT – prepared and analyzed plant extracts and human samples, helped analyze the data, and contributed to the manuscript.

PJW – wrote manuscript, conducted the single human PK test, provided reagents, and helped analyze the data.

REFERENCES:

Arvouet-Grand A, Vennat B, Pourrat A, Legret P. 1994. Standardization of propolis extract and identification of principal constituents. J Pharm Belg 49: 462-468.

Bae JY, Lee GE, Park H, Cho J, Kim YE, Lee JY, Ju C, Kim WK, Kim JI, Park MS. 2020. Pyronaridine and artesunate are potential antiviral drugs against COVID-19 and influenza. bioRxiv. doi: https://doi.org/10.1101/2020.07.28.225102

322 Blasco B, Leroy D, Fidock DA. 2017. Antimalarial drug resistance: linking *Plasmodium falciparum*
323 parasite biology to the clinic. Nat Med 23: 917-928.
324 Cao R, Hu H, Li Y, Wang X, Xu M, Liu J, Zhang H, Yan Y, Zhao L, Li W, Zhang T. 2020. Anti-SARS-CoV-
325 2 potential of artemisinins in vitro. ACS Infect Dis 6: 2524-2531.
326 Desrosiers M, Weathers PJ. 2016. Effect of leaf digestion and artemisinin solubility for use in oral
327 consumption of dried *Artemisia annua* leaves to treat malaria. J Ethnopharmacol 190:313-318.
328 Desrosiers MR, Weathers PJ. 2018. Artemisinin permeability via Caco-2 cells increases after
329 simulated digestion of *Artemisia annua* leaves. J Ethnopharmacol 210: 254-259.
330 Desrosiers MR, Mittelman A, Weathers PJ. 2020. Dried leaf *Artemisia annua* improves
331 bioavailability of artemisinin via cytochrome P450 inhibition and enhances artemisinin efficacy
332 downstream. Biomolecules 10:2:254.
333 Dolivo D, Weathers P, Dominko T. 2020. Artemisinin and artemisinin derivatives as antifibrotic
334 therapeutics. Acta Pharm Sin B, In press. https://doi.org/10.1016/j.apsb.2020.09.001
335 Dow GS, Luttick A, Fenner J, Wesche D, Yeo KR, Rayner C. 2020. Tafenoquine inhibits replication of
336 SARS-Cov-2 at pharmacologically relevant concentrations in vitro. BioRxiv. doi:
337 https://doi.org/10.1101/2020.07.12.199059
338 Efferth T. 2018. Beyond malaria: the inhibition of viruses by artemisinin-type compounds. Biotech
339 Adv 36: 1730-1737.
340 Gendrot M, Duflot I, Boxberger M, Delandre O, Jardot P, Le Bideau M, Andreani J, Fonta I, Mosnier
341 J, Rolland C, Hutter S. 2020. Antimalarial artemisinin-based combination therapies (ACT) and
342 COVID-19 in Africa: In vitro inhibition of SARS-CoV-2 replication by mefloquine-artesunate. Int J
343 Inf Dis 99: 437-440.

344 Gilmore K, Zhou Y, Ramirez S, Pham LV, Fahnoe U, Feng S, Offersgaard A, Trimpert J, Bukh J,
345 Osterrieder K, Gottwein J. 2020. In vitro efficacy of artemisinin-based treatments against SARS-
346 CoV-2. bioRxiv. https://www.biorxiv.org/content/10.1101/2020.10.05.326637v1
347 Hoffmann M, Kleine-Weber H, Schroeder S, Krüger N, Herrler T, Erichsen S, Schiergens TS, Herrler
348 G, Wu NH, Nitsche A, Müller MA, Drosten C, Pöhlmann S. 2020 SARS-CoV-2 cell entry depends
349 on ACE2 and TMPRSS2 and is blocked by a clinically proven protease inhibitor. Cell 181: 271-
350 280.e8.
351 Hunt S, Yoshida M, Davis CE, Greenhill NS, Davis PF. 2015. An extract of the medicinal plant
352 *Artemisia annua* modulates production of inflammatory markers in activated neutrophils. J
353 Inflamm Res 8: 9-14.
354 Hulseberg CE, Fénéant L, Szymańska-de Wijs KM, Kessler NP, Nelson EA, Shoemaker CJ,
355 Schmaljohn CS, Polyak SJ, White JM. 2019. Arbidol and other low-molecular-weight drugs that
356 inhibit Lassa and Ebola viruses. J Virol Apr 3;93: e02185-18.
357 Korber B, Fischer WM, Gnanakaran S, Yoon H, Theiler J, Abfalterer W, Hengartner N, Giorgi EE,
358 Bhattacharya T, Foley B, Hastie KM, Parker MD, Partridge DG, Evans CM, Freeman TM, de Silva
359 TI; Sheffield COVID-19 Genomics Group, McDanal C, Perez LG, Tang H, Moon-Walker A, Whelan
360 SP, LaBranche CC, Saphire EO, Montefiori DC. 2020. Tracking Changes in SARS-CoV-2 Spike:
361 Evidence that D614G Increases Infectivity of the COVID-19 Virus. Cell. Aug 20;182(4):812-
362 827.e19. doi: 10.1016/j.cell.2020.06.043. Epub 2020 Jul 3. PMID: 32697968; PMCID:
363 PMC7332439.
364 Larson SA, Dolivo DM, Dominko T. 2019. Artesunate inhibits myofibroblast formation via induction
365 of apoptosis and antagonism of pro-fibrotic gene expression in human dermal fibroblasts. Cell
366 Bio Int 43:1317-1322.

Lechowicz K, Drożdżal S, Machaj F, Rosik J, Szostak B, Zegan-Barańska M, Biernawska J, Dabrowski W, Rotter I, Kotfis K. 2020. COVID-19: The potential treatment of pulmonary fibrosis associated with SARS-CoV-2 infection. J Clin Med 9:6:1917.

Li SY, Chen C, Zhang HQ, Guo HY, Wang H, Wang L, Zhang X, Hua SN, Yu J, Xiao PG, Li RS. 2005. Identification of natural compounds with antiviral activities against SARS-associated coronavirus. Antiviral Res 67: 18-23.

Liu PP, Blet A, Smyth D, Li H. 2020a. The science underlying COVID-19: implications for the cardiovascular system. Circulation 142: 68-78.

Liu L, Wang P, Nair MS, Yu J, Rapp M, Wang Q, Luo Y, Chan JFW, Sahi V, Figueroa A, Guo XV. 2020b. Potent neutralizing antibodies against multiple epitopes on SARS-CoV-2 spike. Nature 584:(7821):450-456.

Martini MC, Zhang T, Williams JT, Abramovitch RB, Weathers PJ, Shell SS. 2020. *Artemisia annua* and *Artemisia afra* extracts exhibit strong bactericidal activity against *Mycobacterium tuberculosis.* J Ethnopharmacol 262: 113191.

Reed LJ, Muench H. 1938 A simple method of estimating fifty per cent endpoints. Am J Hyg 27:493–497.

Schett G, Sticherling M, Neurath MF. 2020. COVID-19: risk for cytokine targeting in chronic inflammatory diseases? Nat Rev Immunol 20:271-272.

Shi C, Li H, Yang Y, Hou L. 2015. Anti-inflammatory and immunoregulatory functions of artemisinin and its derivatives. Mediators Inflamm 2015:435713.

Spearman, C. 1904. The proof and measurement of association between two things. Am J Psychol 15: 72–101.

389 Towler MJ, Weathers PJ. 2015. Variations in key artemisinic and other metabolites throughout
390 plant development in a clonal cultivar of *Artemisia annua* for possible therapeutic use. Ind Crop
391 Prod 67: 185-191.
392 Uyoga S, Adetifa IMO, Karanja HK, Nyagwange J, Tuju J, Wanjiku P, Aman R, Mwangangi M, Amoth
393 P, Kasera K, Ng'ang'a W, Rombo C, Yegon C, Kithi K, Odhiambo E, Rotich T, Orgut I, Kihara S,
394 Otiende M, Bottomley C, Mupe ZN, Kagucia EW, Gallagher KE, Etyang A, Voller S, Gitonga JN,
395 Mugo D, Agoti CN, Otieno E, Ndwiga L, Lambe T, Wright D, Barasa E, Tsofa B, Bejon P, Ochola-
396 Oyier LI, Agweyu A, Scott JAG, Warimwe GM. 2020. Seroprevalence of anti-SARS-CoV-2 IgG
397 antibodies in Kenyan blood donors. Science 11 Nov 2020
398 http://dx.doi.org/10.1126/science.abe1916
399 Weathers PJ, Arsenault PR, Covello P, McMickle A, Reed D, Teoh KH. 2011. Artemisinin production
400 in *Artemisia annua* - studies in planta and results of a novel delivery method for treating
401 malaria and other neglected diseases. Phytochem Rev 10: 173-183.
402 Weathers PJ, Elfawal MA, Towler, MJ, Acquaah-Mensah G, Rich SM. 2014. Pharmacokinetics of
403 artemisinin delivered by oral consumption of *Artemisia annua* dried leaves (pACT) in healthy vs.
404 *Plasmodium chabaudi*-infected mice. J Ethnopharmacol 153: 732-736.
405 Weathers PJ, Towler MJ. 2014. Changes in key constituents of clonally propagated *Artemisia*
406 *annua* L. during preparation of compressed leaf tablets for possible therapeutic use. Ind Crop
407 Prod 62:173-178.
408 Whitt MA. 2010. Generation of VSV pseudotypes using recombinant ΔG-VSV for studies on virus
409 entry, identification of entry inhibitors, and immune responses to vaccines. J Virol Methods
410 169: 365-74.
411

Table 1. *Artemisia annua* L. cultivars used in the SARS-CoV-2 antiviral analyses.

Cultivar code/ID	Voucher	Yr leaves obtained	Country source	Donor
SAM	MASS 00317314	2020	USA	WPI, originated from F2 generation of PEG01; clonally propagated and grown by Atelier Temenos, Miami , FL
A3 (Anamed A-3)	None *per se*; http://www.anamed-edition.com	2016	Ethiopia	Mary Vanderkooi, Soddo Christian Hospital, Soddo Walaita
PEG01 (PEG01, F2 generation)	None *per se*; Process Engineering Group 01	2008	China	Chunzhao Liu, Chinese Acad Science, Beijing
BUR	LG0019527	2016	Burundi	Ingo Vincens Burow, Savanor, Mutambara, Burundi
MED (Apollon Mediplant)	KL/015/6407	2019	Kenya	Jean Jacques Shul, IDAY, Belgium
FLV5	Artemisia 5 CPMA-UNICAMP 1246	2011	Brazil	Pedro Melillo de Magalhães, CPQBA-UNICAMP, Paulínia-SP
#15	MASS 00317313	Pooled 2013-2015	USA	WPI, originated from F2 generation of PEG01

412

413

414

Table 2. Calculated IC_{50} and IC_{90} values for the 7 *A. annua* cultivars against Vero E6 cells infected with SARS-CoV-2 USA/WA1 (MOI 0.1) based on their measured artemisinin (ART), total flavonoids (tFLV), and dry leaf mass content (DW) in the hot water extracts.

Sample ID	Artemisinin			Total Flavonoids			Dry *A. annua* Leaf Mass		
	ART in tea (µg/mL ± SE)	IC_{50} (µM ART)	IC_{90} (µM ART)	tFLV** (µg/mL ± SE)	IC_{50} (µg)	IC_{90} (µg)	Leaves extracted (g/L)	IC_{50} (µg DW)	IC_{90} (µg DW)
SAM1* (-20C)	149.4 ± 4.4	8.7	18.8	35.4 ± 0.2	0.13	0.28	10	34.9	75.2
SAM2* (4C)	131.6 ± 3.4	5.9	12.3	37.2 ± 0.7	0.14	0.29	10	38.4	79.0
A3	42.5 ± 1.8	1.4	2.7	10.5 ± 0.3	0.03	0.06	10	28.9	54.9
PEG01	82.7 ± 2.8	3.2	13.6	17.6 ± 0.6	0.06	0.25	10	32.9	139.3

FLV5	73.3 ± 2.5	4.9	14.5	7.9 ± 0.1	0.07	0.21	10	57.4	167.8
#15	47.8 ± 2.5	1.8	5.4	10.7 ± 0.2	0.05	0.15	10	32.3	95.7
BUR	20.1 ± 0.8	0.1	0.2	7.3 ± 0.2	0.01	0.03	10	13.5	37.7
MED	59.4 ± 1.6	0.4	1.1	22.3 ± 0.5	0.05	0.13	10	23.4	58.7

* SAM1 and SAM2 are replicated hot water extracts from the same batch of *A. annua* leaves grown and processed from Atelier Temenos; SAM1 was stored at -20C, thawed and reanalyzed at the same time as SAM2. Data are the average of ≥ 6 independently extracted leaf samples.

** Quercetin equivalents.

Table 3. Comparative IC/EC50s for artemisinin derivatives and partner drug antimalarials.

Compound	Cao et al. (2020)	Gilford et al. (2020)	Bae et al. (2020)	This report
	μM			
Artemisinin	64.5	534.8	NM	70
Arteannuin B	10.3	NM	NM	NM
Artemisinic acid	>100	NM	NM	NM
Deoxyartemisinin	NM	NM	NM	>100
Dihydroartemisinin	13.3	NM	NM	>100
Artesunate	13.0	18.2	53, 1.8 (Vero E6, Calu-3)	>100
Arteether	31.9	NM	NM	NM
Artemisone	49.6	NM	NM	NM
Amodiaquine	NM	NM	NM	5.8
Lumefantrine	23.2	NM	NM	NM

NM = not measured

426 **FIGURE LEGENDS**

427 Figure 1. Compounds used in this study and the plant *Artemisia annua* L.

428 Figure. 2. Inhibition plots of extracts for efficacy against Vero E6 cells infected with SARS-CoV-2
429 USA/WA1 (MOI 0.1) based on: artemisinin (A); total flavonoids (tFLV) (B); or dry mass of *A. annua*
430 leaves (C) used in the experiments. Data are plotted from an average of three replicates with ± SE.

431 Figure 3. VSV spike pseudovirus in Calu-3 and Vero E6 cells and their viability in response to
432 increasing hot water *Artemisia* extracts as percent of solvent controls. *Artemisia* concentration
433 refers to dry leaf mass extracted with hot water. Data plotted using nonlinear regression curve
434 fitting using GraphPad Prism. Data are averages of triplicate samples per condition and error bars
435 are ± SD. Data are a representative experiment that was repeated twice.

436 Figure 4. Comparison of *A. annua* SAM extracts and other antimalarial and artemisinin compounds
437 against Vero E6 cells infected with SARS-CoV-2 USA/WA1 (MOI 0.1). A full concentration series for
438 all samples except for the *A. annua* tea could not be fully tested due to solvent toxicity, which was
439 also observed for *A. annua* in dichloromethane (DCM) at higher concentrations. Data are plotted
440 from an average of three replicates with ± SE.

441 Figure 5. Spearman's correlation scatter plots between artemisinin concentration or total
442 flavonoid levels vs. calculated IC_{50} and IC_{90} for the hot water extract of each cultivar from data in
443 Table 2.

444 Figure 6. Cytotoxicity of Vero 6 cells in response to imatinib (A) and *A. annua* hot water extracts
445 (B). Data are plotted from an average of three replicates with ± SE

446

447

448

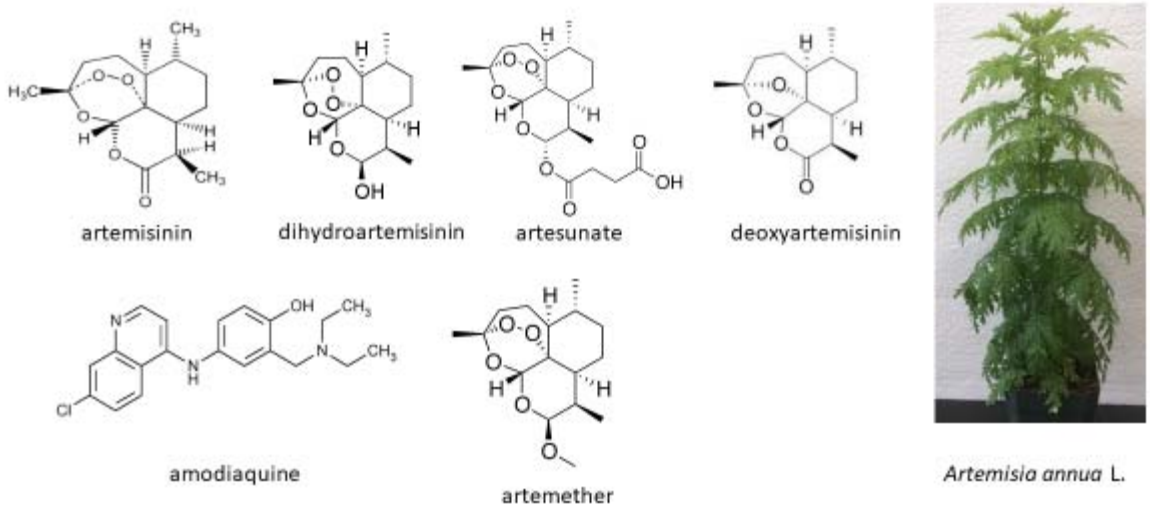

Figure 1. Compounds used in this study and the plant *Artemisia annua* L.

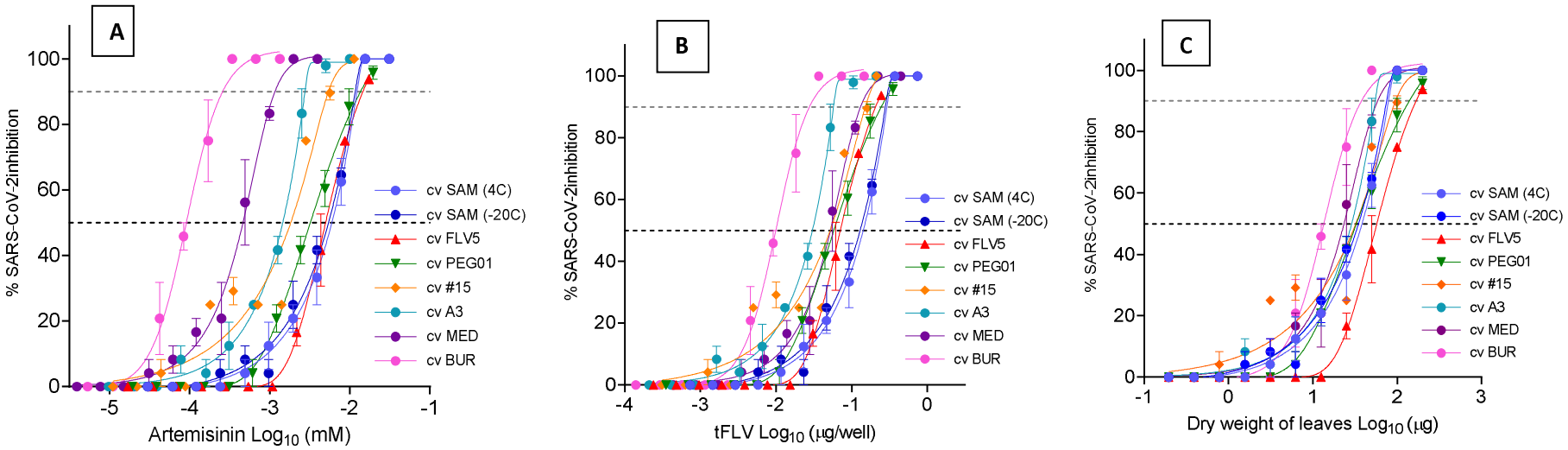

Figure. 2. Inhibition plots of extracts for efficacy against Vero E6 cells infected with SARS-CoV-2 USA/WA1 (MOI 0.1) based on: artemisinin (A); total flavonoids (tFLV) (B); or dry mass of *A. annua* leaves (C) used in the experiments.

468

469

470

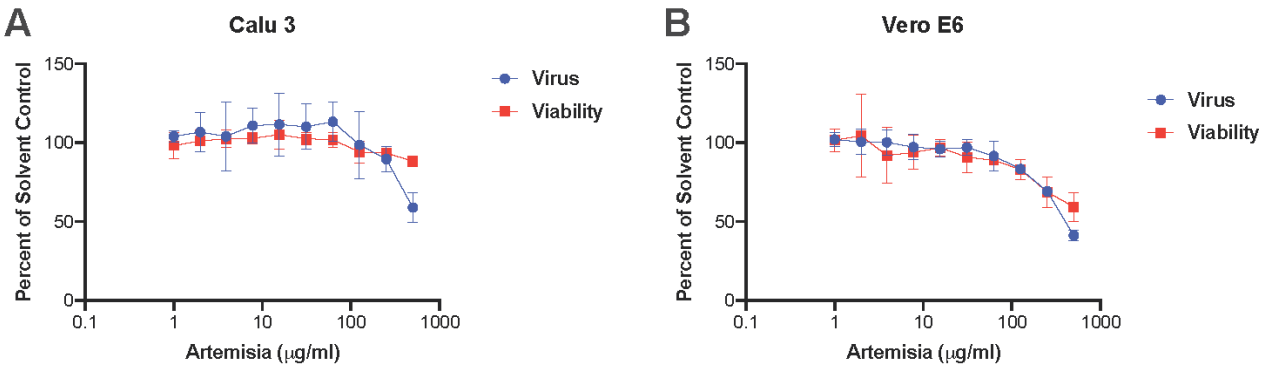

Figure 3. VSV spike pseudovirus in Calu-3 and Vero E6 cells and their viability in response to increasing hot water *Artemisia* extracts as percent of solvent controls. *Artemisia* concentration refers to dry leaf mass extracted with hot water. Data plotted using nonlinear regression curve fitting using GraphPad Prism. Data are averages of triplicate samples per condition and error bars are ± SD. Data are a representative experiment that was repeated twice.

471

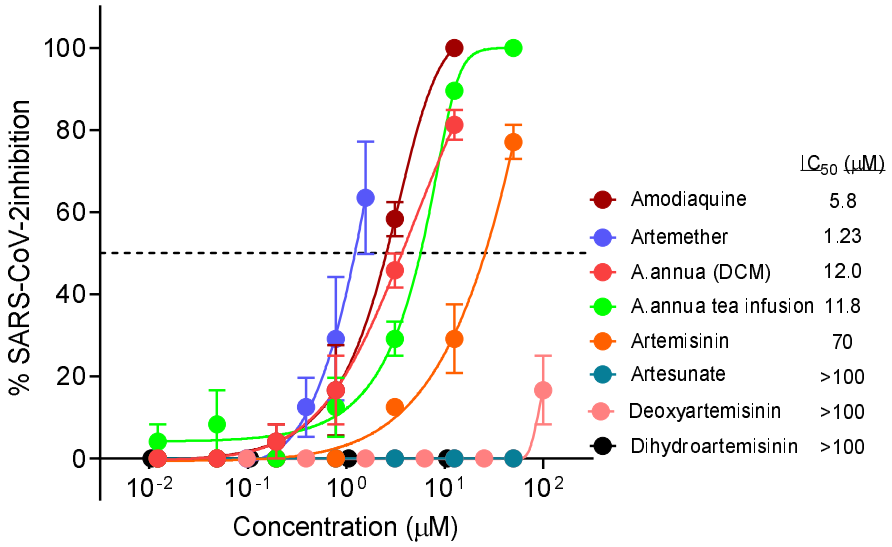

Figure 4. Comparison of *A. annua* SAM extracts and other antimalarial and artemisinin compounds against Vero E6 cells infected with SARS-CoV-2 USA/WA1 (MOI 0.1). A full concentration series for all samples except for the *A. annua* tea could not be fully tested due to solvent toxicity, which was also observed for *A. annua* in dichloromethane (DCM) at higher concentrations.

ARTEMISININ CORRELATIONS

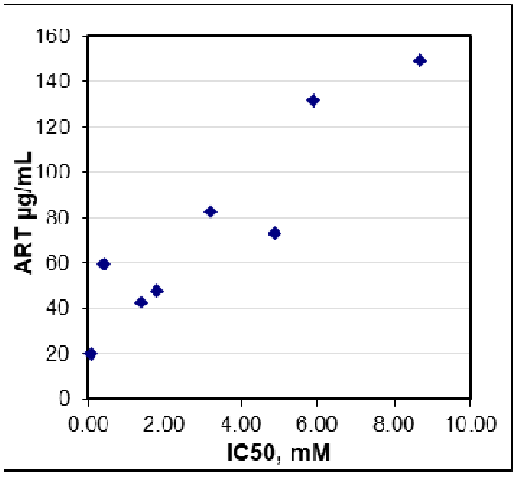

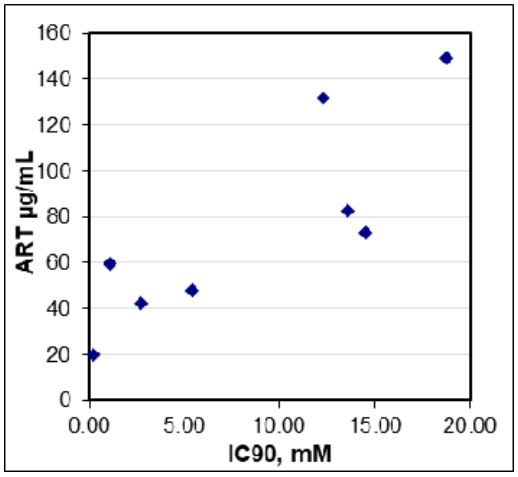

Spearman's Rho=0.90, P=0.002

Spearman's Rho=0.83, P=0.010

TOTAL FLAVONOID CORRELATIONS

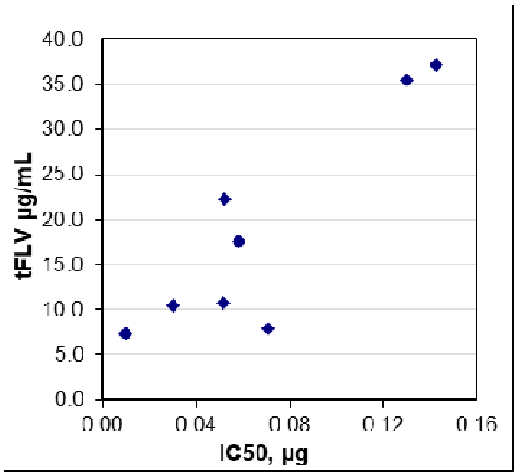

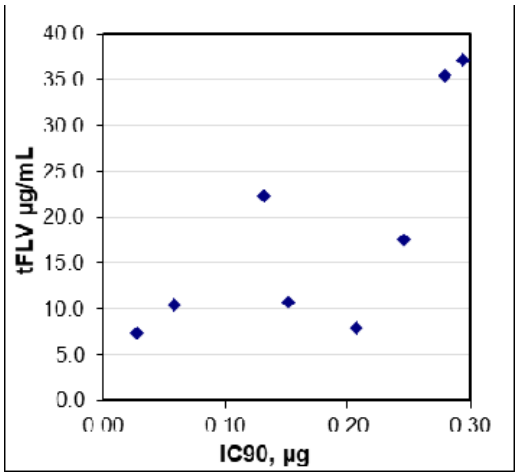

Spearman's Rho=0.74, P=0.037

Spearman's Rho=0.76, P=0.028

Figure 5. Spearman's correlation scatter plots between artemisinin concentration or total flavonoid levels vs. calculated IC_{50} and IC_{90} for the hot water extract of each cultivar from data in Table 2.

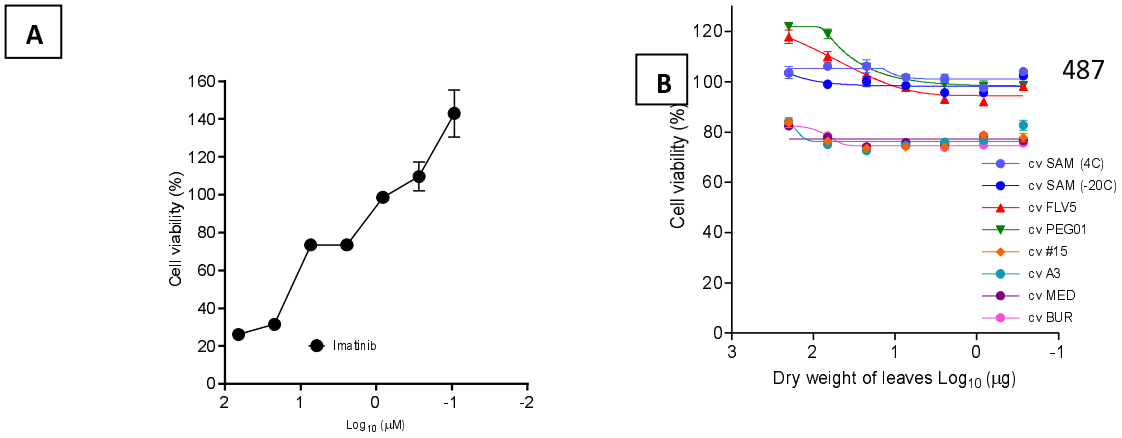

Figure 6. Cytotoxicity of Vero 6 cells in response to imatinib (A) and *A. annua* hot water extracts (B).

Supplemental Data:

Bioavailability of artemisinin from per os consumption of dried leaf Artemisia annua in a human subject.

NB: PJW verified with the WPI IRB that no IRB approval is required for self-experimentation. One of the authors, PJW, age 71, 140 lb [63.6 kg]) consumed 3 g powdered, encapsulated dried *A. annua* SAM (2018 garden crop) and had 3 total blood draws: just prior to consumption; at 2 h post consumption, and a few weeks later, subject took another 3 g dose and blood was drawn 5 h post consumption. Serum was isolated from the blood and analyzed for artemisinin using gas chromatography mass spectrometry (GCMS) per Martini et al. 2020. Artemisinin (MW = 282.33) amount in the encapsulated material was 1.5% (15 mg/g), so amount consumed (delivered) was 45 mg artemisinin. Estimating 100% bioavailability, and that this human subject had a total volume of about 4.13 L blood (https://reference.medscape.com/calculator/estimated-blood-volume), the amount of delivered artemisinin/mL blood could not exceed 10.90 mg/L, or 10.90 µg/mL. Human blood is 55% serum (or 2.3 L for this human subject), so the highest serum concentration of artemisinin would actually be about 20 mg/L or 20 µg/mL.

Table S1. Human pharmacokinetics of ART delivered from *p.o. Artemisia annua*.[a]

Time (h)	ART in serum (µg/mL)	% of *A. annua*-ART consumed
0	0.0	0
2	7.04	36
5	0.16	0.8

[a] Consumed 3 g powdered dried leaf *A. annua* containing 10.90 mg ART *in toto;* maximum possible serum concentration at *p.o.* delivery = 19.62 µg ART/mL.

Table S2. Examples of comparative amounts of artemisinin metabolites in various cultivars of *A. annua*.

Compound	LUX MNHNL17732	BUR LG0019527	SAM1,[1] MASS 00317314
	mg/g dry weight leaves		
Artemisinin	1.34	1.70	10.94[2],15.90[1]
Arteannuin B	0.93	ND	0.09[2], 2.32[1]
Artemisinic acid	0.86	ND	ND[2], 0.37[1]
Deoxyartemisinin	0.32	0.39	0.83[2], NM[1]

ND, not detected; NM, not measured.

[1] Data from Weathers and Towler (2014) Ind Crop Prod 62:173-178; artemisinic acid is detectable in the dried leaves.

533 [2] Data estimated from fresh leaf analysis using dry weight/fresh weight ratio = 0.26 from Table 1 in

534 Towler and Weathers (2015) Ind Crop Prod 67:185-191.

535

536